Tropospheric Ozone and Climate: Past, Present and Future

Guy P. Brasseur[1,3], Jean-Francois Müller[2],
XueXi Tie[3] and Larry Horowitz[4]

[1]*Max Planck Institute for Meteorology, Hamburg, Germany*
[2]*Belgian Institute for Space Aeronomy, Brussels, Belgium*
[3]*National Center for Atmospheric Research, Boulder, Colorado, U.S.A.*
[4]*NOAA Geophysical Fluid Dynamics Laboratory, Princeton, New Jersey, U.S.A.*

Abstract—The paper describes the major processes that contribute to the distribution of ozone in the global troposphere. It briefly reviews the components of the tropospheric ozone budget, including the photochemical mechanisms that lead to in situ production and destruction of ozone. A simplified three-dimensional chemical transport model (IMAGES) is used to calculate the changes in the global abundance of ozone and its precursors since the pre-industrial era, and to assess how the concentration of these gases could change in the future in response to expected changes in human activities.

INTRODUCTION

Early climate models designed to assess the impact of human activities on the climate system focused primarily on the impact of carbon dioxide (CO_2). This gas, whose atmospheric abundance has increased by 30% since the pre-industrial era, is known to trap a fraction of the radiative energy emitted by the surface-atmosphere system, and hence to contribute to the so-called "greenhouse effect". The effects of other "well-mixed" greenhouse gases including methane (CH_4), nitrous oxide (N_2O) and various chlorofluorocarbons (CFCs), whose atmospheric concentrations have also been increasing with time have been considered in more recent model studies (Bengtsson *et al.*, 1999). Modern climate models also include the radiative effects of aerosol particles and ozone (O_3). Sulfate particles (SO_4), for example, are known to scatter a fraction of the incoming solar radiation back to space, and hence to cool the planet. By modifying the optical properties and the lifetime of clouds, these particles also produce an indirect cooling effect on climate, which remains poorly quantified. Other aerosols, such as soot particles, absorb some of the incoming solar radiation, leading to a warming effect.

Atmospheric ozone interacts with solar as well as terrestrial radiation. By absorbing ultraviolet and visible solar light, it heats the middle atmosphere, where its concentration is highest. At the same time, through its strong absorption band at 9.6 microns, it traps some of the terrestrial radiation, a process that tends to warm up the Earth's surface. The largest contribution to this "greenhouse"

warming is provided by ozone located in the vicinity of the tropopause where the temperature is considerably lower than near the surface (Lacis *et al.*, 1990). Ozone depletion in the lower stratosphere (for example as a result of CFC emissions) is therefore expected to produce a cooling of the lower stratosphere, while an ozone build-up in the upper troposphere (for example as a result of nitric oxide emissions from subsonic aircraft) should contribute to the warming of the planet.

Ozone plays several environmentally important roles in addition to its influence on the climate system. First, by absorbing solar ultraviolet radiation, it protects the biosphere from harmful effects. Its destruction in the stratosphere could lead to a substantial increase in the incidence of skin cancer among the human population. Second, as a strong oxidant and, together with water vapor, as a precursor of the hydroxyl radical (OH), ozone has a strong influence on the "oxidizing power" of the atmosphere and hence on the rate at which many natural and anthropogenic compounds are eliminated from the atmosphere. A human-induced reduction in the oxidizing power of the atmosphere could indirectly affect climate since greenhouse gases like methane (which are primarily destroyed by OH) would more easily accumulate in the atmosphere. Such feedbacks need to be included in modern state-of-the-art climate models.

OZONE CHEMISTRY

Approximately 90% of the ozone in the atmosphere is located in the middle atmosphere (15–100 km), where it is produced as a result of molecular oxygen photolysis by solar ultraviolet radiation. The destruction of ozone in this atmospheric region results from a reaction with atomic oxygen, itself produced by O_3 photolysis (Chapman, 1930). This destruction mechanism, however, is too slow to explain the observed ozone concentration in the middle atmosphere, so that other chemical processes need to be invoked. Laboratory studies have shown that ozone can be efficiently destroyed by catalytic reactions involving the presence of hydrogen radicals (Bates and Nicolet, 1950), nitrogen oxides (Crutzen, 1973), chlorine atoms (Stolarski and Cicerone, 1974) and bromine atoms (Wofsy *et al.*, 1975). The source of these catalysts is provided by long-lived natural or anthropogenic molecules originating in the troposphere and being transported to the stratosphere. Chlorine atoms, for example, are provided primarily by the photodecomposition of industrially manufactured chlorofluorocarbons. Such products have been identified as a major threat to the ozone layer in the upper stratosphere, and are probably responsible for most of the observed ozone depletion recorded by satellite and ground-based instrumentation.

In the mid-1980s it became obvious that additional mechanisms had to be introduced to explain the decline of ozone observed in the lower stratosphere. This became particularly obvious after the ozone hole (which had not been predicted by early atmospheric models) was repeatedly observed each austral spring (September to November) over the Antarctic continent. Laboratory measurements as well as field observations suggested that slow-reacting inorganic

chlorine and bromine reservoirs could be converted into more reactive forms through reactions on the surface of liquid or solid aerosol particles. The presence of stratospheric clouds present in the polar lower stratosphere provides sites on which such chlorine activation can occur. When the Sun returns in the polar regions, large amounts of ozone can be destroyed by the activated chlorine. Substantial ozone depletion can also occur at mid- and high latitudes in response to the enhancement of the stratospheric sulfate aerosol load following a major volcanic eruption.

Until the beginning of the 1970s, it was believed that the presence of ozone in the troposphere was due primarily to the downward transport of ozone-rich airmasses through the tropopause, since the ultraviolet radiation required to photolyze molecular oxygen and produce ozone was entirely absorbed in the stratosphere. In the early 1950s, however, it had been shown that the high levels of ozone frequently observed during daytime in large metropolitan areas like Los Angeles were due to local photochemical production involving the oxidation of hydrocarbons (released for example in automobile exhaust) in the presence of nitrogen oxides. In the early 1970s, Crutzen (1973) and Chameides and Walker (1973) suggested that similar reactions could play an important role throughout the entire troposphere. The primary "fuels" present in the atmosphere away from urbanized and industrialized areas are carbon monoxide and methane. For sufficiently high levels of nitrogen oxides present (i.e., in weakly polluted areas), the oxidation of these "fuels" leads to ozone formation, while for low concentrations of nitrogen oxides (i.e., over oceans), ozone is destroyed.

The presence in the troposphere of nitrogen oxides, carbon monoxide and various hydrocarbons also affects the concentration of the OH radical and therefore the oxidizing power of the atmosphere. In most regions of the atmosphere, the formation of OH results primarily from the photolysis of ozone, producing an electronically excited oxygen atom, followed by the reaction of this atom with water vapor. Additional production mechanisms, important in the tropical upper troposphere, involve the presence of organic compounds (such as acetone and peroxides) transported from the boundary layer in convective systems. The concentration of hydroxyl radicals is also affected by other atmospheric compounds: carbon monoxide converts OH into the hydroperoxy radical HO_2, while nitric oxide converts HO_2 back to OH. The reactions involved in the formation and destruction of ozone therefore affect the concentrations of OH and HO_2.

Ozone precursors such as NO_x, CO, CH_4 and nonmethane hydrocarbons (NMHC) are present in the troposphere under natural conditions. For example, nitrogen oxides are produced by lightning in convective clouds and are released by microbial processes in soils. Carbon monoxide is produced by the oxidation of methane and methane itself is released by wetlands. Other organic compounds such as isoprene are emitted by vegetation. These compounds are also produced as a result of human activities. NO_x and CO are both a product of combustion and are therefore released in the atmosphere as a result of fossil fuel combustion and

Table 1. Contemporary Surface Emissions used in IMAGES (Müller, 1992).

	Technological source	Biomass burning	Biogenic[1]	Oceans	Total Tg
NO_x-N	59%	15%	18%	1·E-6	37[2]
SO_2-S	100%				91[3]
DMS				100%	21
CO	27%	51%	11%	11%	1440[4]
CH_4	26%	11%	61%	2%	506[4]
VOCs	13%	7%	67%	13%	750[4]

[1]Includes animal, microbial and foliage emissions.
[2]Tg N.
[3]Tg S.
[4]Tg CO, CH_4, or VOCs respectively.

biomass burning. Methane is released from coal mines and from rice paddies. Table 1 shows an estimate of the total present-day emissions of several important ozone precursors, and highlights the natural and anthropogenic contributions. It is clear from this table that the atmospheric concentration of most ozone precursors (and therefore of ozone itself) should have increased dramatically in response to human activities.

Trends in tropospheric ozone are poorly documented. Early observations, using the relatively crude technique of the Schoenbein paper, suggest that surface ozone concentrations at the late 19th century were of the order of 10–20 ppbv even in an urban area such as that of the Parc Montsouris in Paris (Volz and Kley, 1988). Such values are considerably lower than present-day background concentration values (typically 40–50 ppbv) observed over the continents in the Northern hemisphere. During pollution episodes, ozone mixing ratios higher than 80 ppbv can be observed locally in the industrialized regions of North America, Europe and Asia. It is likely that, on the average, the ozone abundance in the Northern hemisphere has increased by a factor of 2 or more since the pre-industrial era (WMO, 1999), and it is therefore conceivable that the oxidizing power of the atmosphere has changed during the same period. Since no data is available to estimate the true change in the average OH density, only models can provide quantitative estimates. A recent analysis of methyl chloroform data gathered at different stations has provided some information on the likely changes in the mean OH density during the last 2 decades (Prinn *et al.*, 1992).

THE IMAGES MODEL

In order to assess past and future changes in the tropospheric ozone concentration, we use a three-dimensional chemical transport model, called IMAGES (Intermediate Model for the Annual and Global Evolution of Chemical Species). This model is described in detail and evaluated by Müller and Brasseur (1995), so that little further information will be given here. Like most chemical
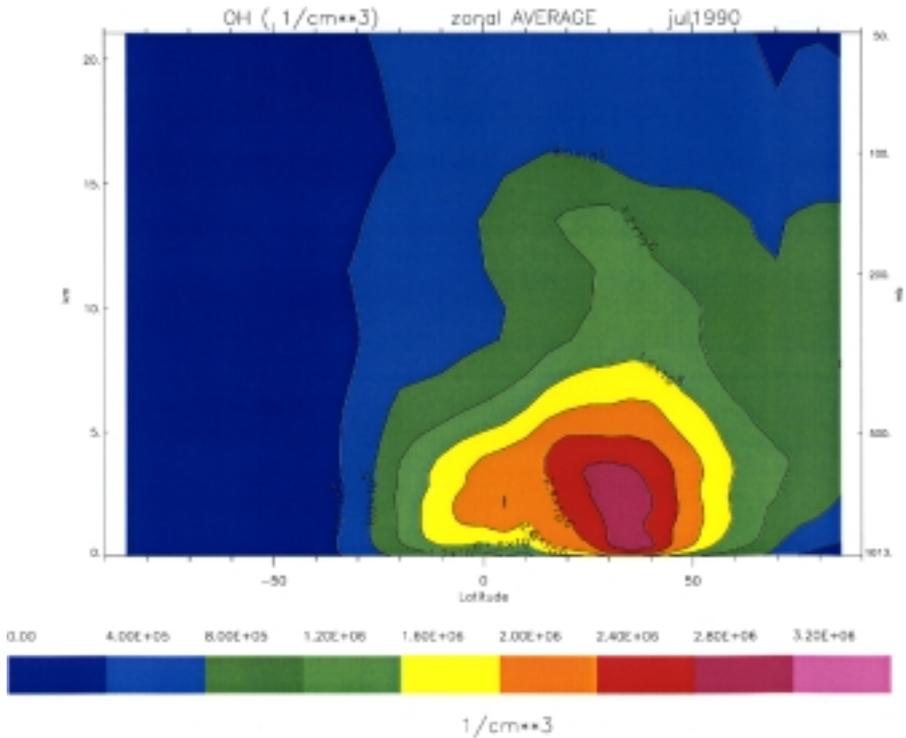
Fig. 1. Global distribution of the July monthly mean ozone mixing ratio (ppbv) calculated by the
IMAGES model on the sigma = 0.7 surface level (approximately 2.5 km altitude over the ocean)
for 1990 conditions.

transport models, IMAGES incorporates several basic elements: surface emissions, large-scale atmospheric transport, subscale dynamical exchanges, chemical transformations, and surface deposition. The model extends from pole to pole, and from the surface to the lower stratosphere (50 hPa) with 25 terrain-following levels (sigma coordinates). The horizontal resolution is 5° in longitude and latitude and the transport time step is 6 hours. Transport is driven by "climatological" winds derived from the analyses provided by the European Center for Medium-Range Weather Forecast (ECMWF). The model simulates advection using a semi-Lagrangian transport algorithm (Smolarkiewicz and Rasch, 1991), and accounts for sub-grid transport through diffusive mixing in the boundary layer, deep convection (Costen *et al*., 1988) in the free troposphere, and eddy diffusive mixing to account for unresolved wind variability. IMAGES derives the concentrations of 41 species including 7 different primary hydrocarbons and several oxygenated organic species. It accounts for 125 reactions (including 26 photolytic reactions and several heterogeneous reactions). Wet deposition is parameterized as a first-order loss rate calculated as a function of the precipitation

Fig. 2. Zonally averaged OH number density (cm^{-3}) calculated for July 1990.

rate, taken from the climatology of Shea (1986). This formulation accounts for the different types of precipitation and for species dependent solubility. Dry deposition is expressed using vegetation specific deposition velocities, which vary considerably from species to species. Surface emissions (biogenic and anthropogenic sources) are prescribed, based on estimates by Müller (1992) and several more recent updates. The atmospheric production of nitrogen oxides associated with lightning and commercial aircraft operations is included in the model. The pre-industrial atmosphere is represented by omitting the emissions of chemical compounds produced by fossil fuel consumption and by arbitrarily reducing by a factor of 3 the emissions associated with biomass burning. The future atmosphere is simulated on the basis of the IS92a scenario developed for IPCC 1995. In both the pre-industrial and future cases, the atmospheric dynamics, temperature, and water vapor concentration are assumed to be the same as for the present. The consequences of this approximation need to be further investigated.

      In the following sections, model results will be shown for July, when photochemical conditions are most active in the Northern hemisphere. The calculated fields will be displayed either as zonal mean (shown as a function of
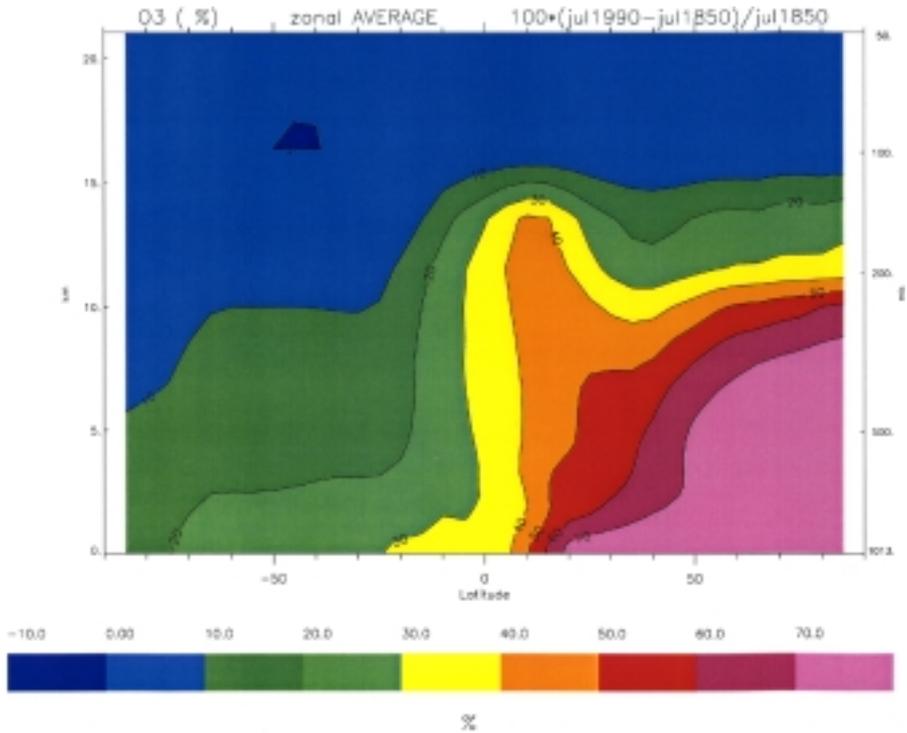
Fig. 3. Relative change (percent) in the July zonally averaged ozone concentration between the pre-industrial era (1850) and the contemporary period (1990).

latitude and height) or on the sigma = 0.7 surface. This terrain-following surface (which corresponds to a pressure surface of 700 hPa over the oceans) is generally located slightly above the planetary boundary layer and provides conditions that are representative of the lower part of the free troposphere.

In order to illustrate the results provided by the model, we first present selected results from our simulation of present-day conditions. For this purpose, the model is integrated for a period of 2 years, a time period that is sufficiently long for chemically active species to reach equilibrium conditions. In the case of long-lived tracers like methane (lifetime of about 8 years), the initial concentrations and hence the model solutions are representative of present-day values.

Figure 1 shows the global distribution of the ozone mixing ratio (monthly mean) calculated by IMAGES for July (1990 conditions) on the sigma = 0.7 level. The calculated values are typically 30–40 ppbv in the Southern hemisphere and 40–50 ppbv in the Northern hemisphere, with higher values predicted in specific areas. One of these areas is located in the southern tropics, and is associated with the large NO_x emissions from lightning and biomass burning over the tropical continents. In these regions, the ozone mixing ratios just above the top of the
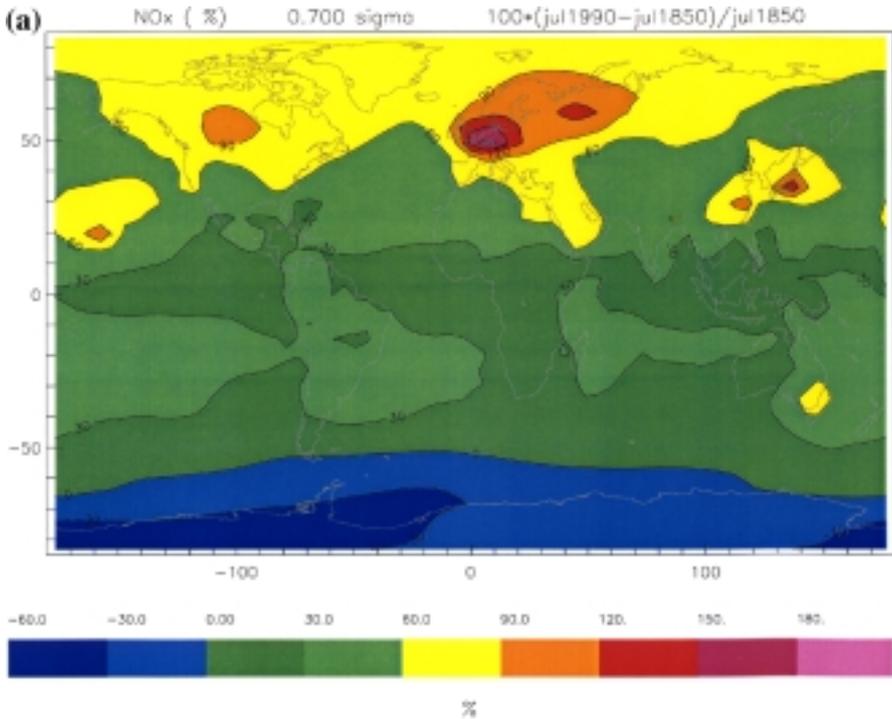
Fig. 4. Relative change (percent) in the concentration of (a) nitrogen oxides (NO_x) and (b) ozone (O_3) on the sigma = 0.7 surface level (approximately 2.5 km altitude over the ocean) in July between 1850 and 1990.

boundary layer are typically 50–60 ppbv. A second area with high ozone values (50–60 ppbv) is found at northern mid-latitudes (North America, Europe and Asia) where anthropogenic emissions of ozone precursors are high. Note that the high ozone mixing ratios calculated near the Himalayas are due in large part to the fact that the sigma surfaces reach relatively high altitudes in this region. The lowest ozone concentrations (10–20 ppbv) are found in the tropics over the Pacific ocean.

As indicated above, an important quantity for the chemistry of the troposphere is the abundance of the hydroxyl (OH) radical. Its zonally averaged number density in July, as calculated by IMAGES, is represented in Fig. 2. During July, the maximum OH density ($28 \cdot 10^5$ cm^{-3} below 5 km altitude) is displaced from the equator towards northern mid-latitudes (35°N). Values in the winter hemisphere poleward of 40° are less than $4 \cdot 10^5$ cm^{-3}, so that the oxidation power of the atmosphere in these regions is very small. The global methane and methyl chloroform lifetimes calculated with the OH fields provided by IMAGES are 8.3 and 4.2 years, respectively.
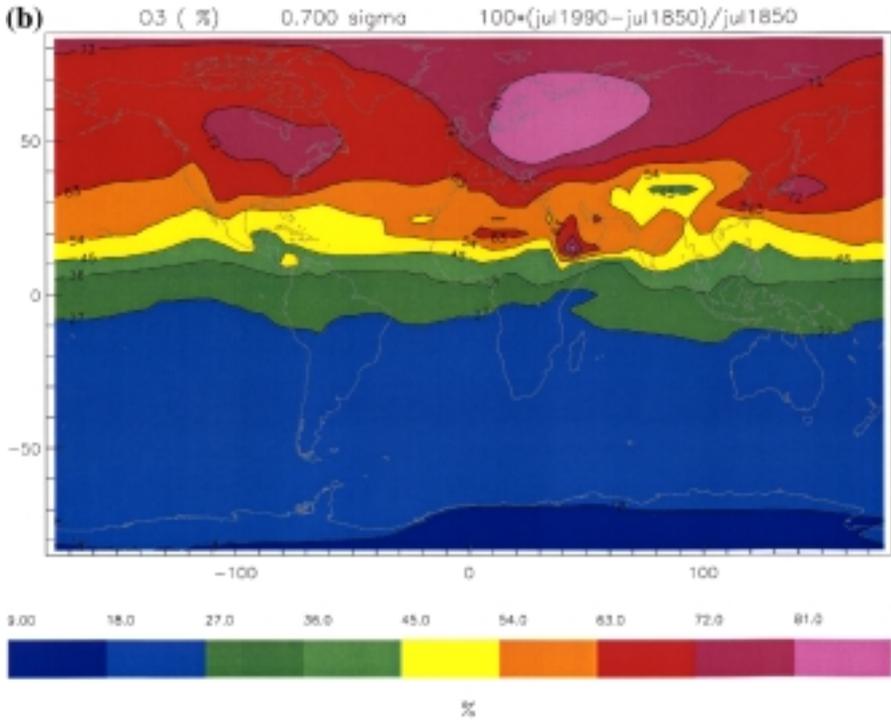
Fig. 4. (continued).

CALCULATED CHANGES IN THE CHEMICAL COMPOSITION SINCE THE PRE-INDUSTRIAL ERA

In this section, we present a model estimate of the changes that may have occurred in the chemical composition of the global troposphere since the pre-industrial era. As the conditions regarding the surface emissions during the 19th century are poorly known, the calculated concentrations for that period (and hence the change during the last 150 years) are rather uncertain. A major uncertainty in deriving the pre-industrial levels of ozone results from our poor knowledge of biomass burning intensity during the 19th century. Figure 3 presents a model estimate of the change in the ozone mixing ratio between 1850 and 1990, based on the assumptions stated above. It shows that the zonal mean ozone abundance in July has increased by more than 70% in the northern mid- and high latitudes and by 40% in the subtropics. The changes in the southern hemisphere during July are between 10 and 30%. It is interesting to point out that the impact of human activities is visible not only near the surface but all the way to the tropopause. Ozone changes are therefore expected to affect climate significantly. Looking more specifically at the changes in ozone and its precursors
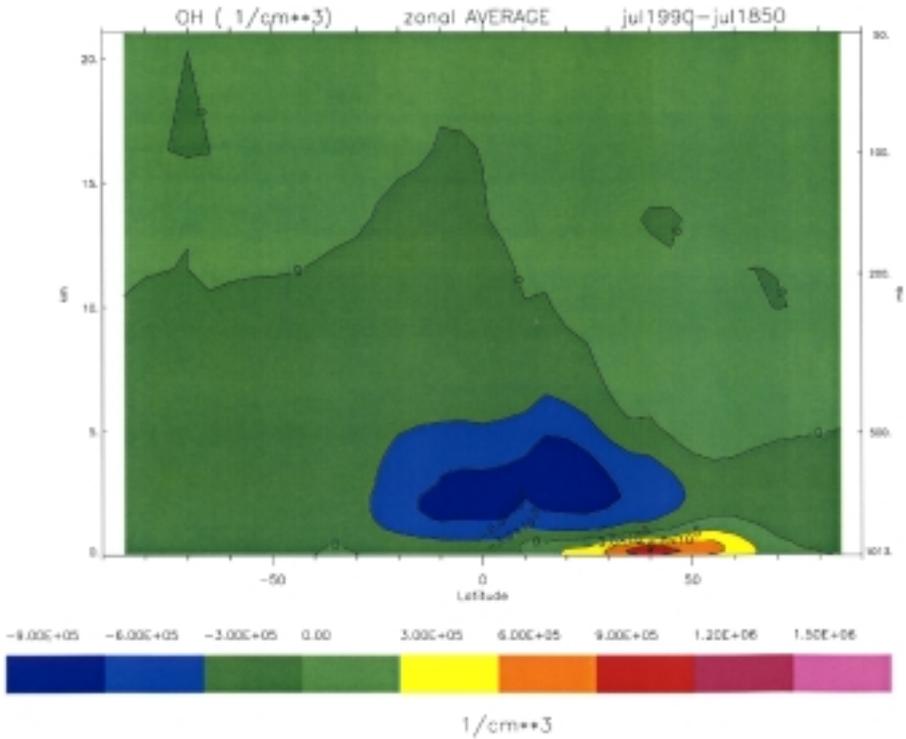
Fig. 5. Absolute change (cm^{-3}) in the zonally averaged concentration of the hydroxyl (OH) radical between 1850 and 1990 calculated for July conditions.

on the sigma = 0.7 level (Figs. 4a and b), one sees that the ozone changes in the lower part of the free troposphere are relatively evenly distributed in the northern hemisphere, with slightly enhanced values, however, above the industrialized areas. These somewhat higher values correspond to maximum changes in the NO_x concentrations (more than 80%) over North America, Europe, China and Japan. Note the small changes in NO_x densities in the tropics and subtropics with exceptions in regions where biomass burning has increased substantially. At the surface (not shown), the changes in the ozone abundance are much less uniform in space; they reach typically 100–150% in regions where intense industrialization and urbanization took place.

An important issue is to assess the possible change in the mean OH abundance since the pre-industrial era, as this quantity provides an indication of the change in the oxidation potential of the atmosphere in response to human activities. An accurate calculation of this effect is not straightforward, since several processes with opposite effects on ozone are taking place simultaneously.
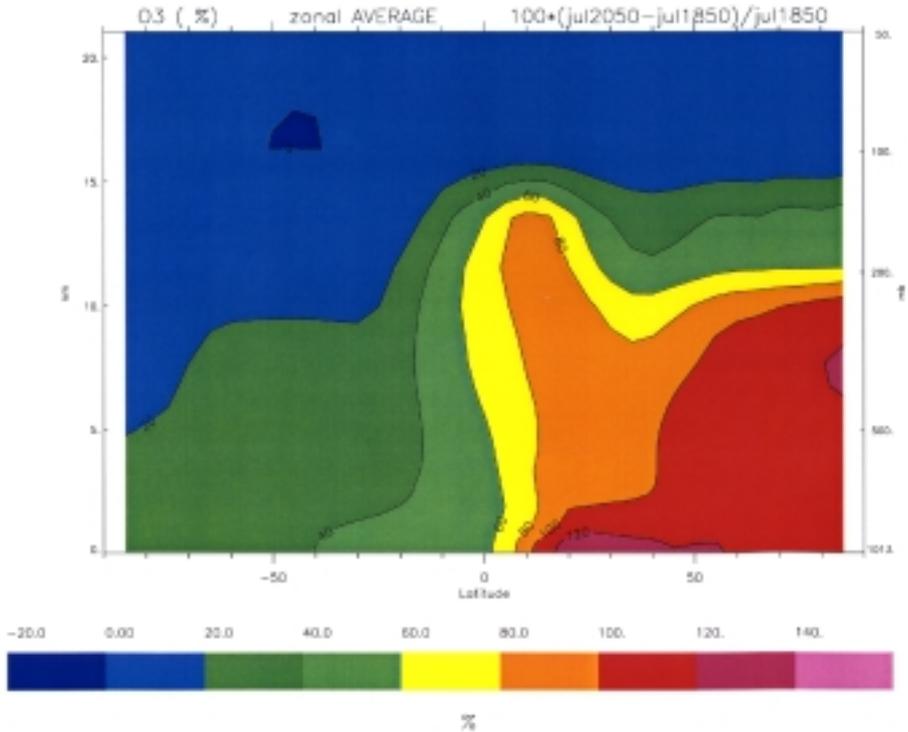
Fig. 6. Relative change (percent) in the zonally averaged ozone concentration estimated for the 1850–2050 period on the basis of the IPCC IS92a scenario (July conditions).

Figure 5 shows an estimate of this perturbation. The IMAGES model suggests that the average OH concentration has decreased in the free troposphere, primarily as a result of the increase in carbon monoxide concentrations. A reduction of $(5-8) \cdot 10^5$ cm^{-3} is calculated at 2–3 km in the tropics (between 10°S and 30°N) where the mean OH density ranges typically from $18 \cdot 10^5$ to $28 \cdot 10^5$ cm^{-3}. In the boundary layer of the northern hemisphere, the concentration of OH increases due primarily to enhanced conversion of HO_2 to OH by elevated concentrations of NO_x. Nitrogen oxides have a considerably shorter lifetime than carbon monoxide. Therefore, the NO_x effect (leading to OH increase) dominates near the emissions sources while that of CO (leading to OH decrease) provides the largest influence in the free troposphere. The net effect is a reduction in the globally averaged OH density. Based on the IMAGES calculations, the mean lifetimes of methane and methylchloroform (respectively 8.9 and 4.8 years for present-day conditions, see WMO, 1999) have increased since the pre-industrial era by approximately 1.3 year and 7 months, respectively.

ESTIMATED FUTURE CHANGES IN THE CHEMICAL COMPOSITION OF THE GLOBAL TROPOSPHERE

Finally, we show model predictions of possible changes in future ozone concentrations. As stated earlier, this calculation is based on a particular emission scenario proposed by IPCC (IS92a). Figure 6 shows an estimate of the changes in the zonally averaged ozone concentrations between the years 1850 and 2050. The model suggests for this period of 200 years an ozone increase of 100–120% in the northern mid-latitudes during July and of 80–100% in the tropics. Large changes are noticeable near the tropopause where the ozone changes have a substantial impact on climate forcing. When comparing to the present-day situation (not shown), the predicted ozone increase by 2050 is typically 25–30% in the tropics (surface to 15 km altitude). These changes reflect the rapid economic growth expected in these regions and specifically in South and Southeast Asia and, to a lesser extent, in Central and South America. At mid- and high latitudes (July), the changes calculated from present-day to year 2050 range from 15–30%, with the maximum relative perturbation occurring around 8–12 km in response to projected increases in NO_x emissions from commercial aircraft. Further changes are also expected for OH; over the 1990–2050 period, the estimated lifetimes of methane and methylchloroform are further enhanced by 6 months and 2 months, respectively.

CONCLUDING REMARKS

The chemical composition of the global atmosphere, and more specifically the abundance of ozone and its precursors have most likely changed dramatically since the pre-industrial era. Model calculations show that near the surface, the changes have been largest in Europe, North America and eastern Asia, due to increasing consumption of fossil fuel. In the middle and upper troposphere, the ozone changes are found to be spread relatively uniformly over the entire Northern hemisphere. Aviation has directly contributed to these large-scale perturbations. The globally averaged radiative forcing produced by the changes in ozone is estimated to be approximately 0.4 Wm^{-2} (Brasseur *et al.*, 1998), with regional effects reaching almost 1 Wm^{-2}. Such perturbations cannot be ignored, when compared to climate forcing resulting from the increase (since the pre-industrial era) in the concentration of well-mixed greenhouse gases or from changes in the atmospheric aerosol load.

When considering projected changes to be expected over the next 50 years on the basis of the IS92a scenario of IPCC, the model suggests that most changes in the abundance of surface ozone will take place in the tropics, and specifically in south Asia (India, China). Significant perturbations should also be expected in Central and South America as well as southern Africa. The impact on ozone near the tropopause of the assumed growth in commercial aviation and related emissions should also be substantial. The calculated globally averaged radiative forcing (0.25 Wm^{-2}) is somewhat lower than that estimated for the past 150 years. Estimates of future changes depend crucially on the level and type of economic

development assumed in the adopted scenarios. Large uncertainties are therefore associated with model predictions for the future.

REFERENCES

Bates, D. R. and M. Nicolet, Photochemistry of water vapor, *J. Geophys. Res.*, **55**, 301–327, 1950.

Bengtsson, L., E. Roeckner, and M. Stendel, Why is the global warming proceeding much slower than expected?, *J. Geophys. Res.*, **104**, 3865–3876, 1999.

Brasseur, G. P., J. T. Kiehl, J. F. Müller, T. Schneider, C. Granier, X. X. Tie, and D. Hauglustaine, Past and future changes in global tropospheric ozone: Impact on radiative forcing, *Geophys. Res. Lett.*, **25**, 3807–3810, 1998.

Brasseur, G. P., J. J. Orlando, and G. S. Tyndall, *Atmospheric Chemistry and Global Change*, Oxford University Press, 654 pp., 1999.

Chameides, W. L. and J. C. G. Walker, A photochemical theory of tropospheric ozone, *J. Geophys. Res.*, **78**, 8751–8760, 1973.

Chapman, S., A theory of upper atmospheric ozone, *Memoirs Roy. Met. Soc.*, **3**, 103–125, 1930.

Costen, R. C., G. M. Tennille, and J. S. Levine, Cloud pumping in a one-dimensional model, *J. Geophys. Res.*, **93**, 941–954, 1988.

Crutzen, P. J., The influence of nitrogen oxides on the atmospheric ozone content, *Quart. J. Roy. Meteorl. Soc.*, **96**, 320, 1970.

Crutzen, P. J., A discussion of the chemistry of the stratosphere and troposphere, *Pure Appl. Geophys.*, **106–108**, 1385–1399, 1973.

IPCC, *Climate Change 1995*, Cambridge University Press, Cambridge, 1996.

Lacis, A. A., D. J. Wuebbles, and J. A. Logan, Radiative forcing by changes in the vertical distribution of ozone, *J. Geophys. Res.*, **95**, 9971–9981, 1990.

Müller, J. F., Geographical distribution and seasonal variation of surface emissions and deposition velocities of atmospheric trace gases, *J. Geophys. Res.*, **97**, 3787–3804, 1992.

Müller, J. F. and G. Brasseur, IMAGES: A three-dimensional chemical transport model of the global troposphere, *J. Geophys. Res.*, **100**, 445–490, 1995.

Prinn, R., D. Cunnold, P. Simmonds, F. Alyea, R. Boldi, A. Crawford, P. Fraser, D. Gutzler, D. Hartley, R. Rosen, and R. Rasmussen, Global average concentration and trend for hydroxyl radicals deduced from ALE/GAGE trichloroethane (methyl chloroform) data for 1978–1990, *J. Geophys. Res.*, **97**, 2445–2461, 1992.

Shea, R. C., Climatological Atlas: 1950–1979, NCAR Technical Note, NCAR/TN-269+STR, 1986.

Smolarkiewicz, P. K. and P. J. Rash, Monotone advection on the sphere: An Eulerian versus semi-Langrangian approach, *J. Atmos. Sci.*, **48**, 793–810, 1991.

Stolarski, R. S. and R. J. Cicerone, Stratospheric chlorine: A possible sink for ozone, *Can. J. Chem.*, **52**, 1610–1615, 1974.

Volz, A. and D. Kley, Evaluation of the Montsouris series of ozone measurements made in the nineteenth century, *Nature*, **332**, 240–242, 1988.

WMO, Scientific Assessment of Ozone Depletion: 1998. Global Ozone Research and Monitoring Project—Report No. 44. World Meteorological Organization, Geneva, 1999.

Wofsy, S. C., M. B. McElroy, and Y. L. Yung, The chemistry of atmospheric bromine, *Geophys. Res. Lett.*, **2**, 215–218, 1975.

G. P. Brasseur (e-mail: brasseur@dkrz.de), J.-F. Müller, X-X. Tie and L. Horowitz